

- (28) Dehl, R. E. *J. Chem. Phys.* **1968**, *48*, 831.
 (29) Schneider, W. G., footnote 75, ref 26.
 (30) von Meerwall, E.; Ferguson, R. D. *J. Polym. Sci.*, in press.
 (31) Samulski, E. T. *J. Phys. Colloq.* **1979**, *40*, C3-471.
 (32) Poupko, R.; Luz, Z.; Samulski, E. T. *J. Chem. Phys.*, in press.
 (33) Translational diffusion constants for the solvent in the swollen network are within an order of magnitude of that of the pure solvent: von Meerwall, E.; Ferguson, R. D. *J. Appl. Polym. Sci.* **1979**, *23*, 877, 3657. This implies that on the ^2H NMR time scale ($t > 10^{-5}$ s), the swelling agent probes macroscopic distances within the network, much larger than the chain dimensions.
 (34) Brochard, F. *J. Phys. (Paris)* **1979**, *40*, 1049.
 (35) de Gennes, P. G. "Scaling Concepts in Polymer Physics"; Cornell University Press: Ithaca, N.Y., 1979; p 158.
 (36) Stephen, M. J.; Straley, J. P. *Rev. Mod. Phys.* **1974**, *46*, 618.
 (37) Roe, R. J.; Krigbaum, W. R. *J. Appl. Phys.* **1964**, *35*, 2215.
 (38) See ref 1, p 179.
 (39) The quadrupolar splitting for CDCl_3 shown in Figure 2 yields a value of S_{zz} that is a factor of 1.5 larger than that observed for C_6D_6 (after including the differences in θ_i and $(e^2qQ/h)_i$) constrained in the same network under the same conditions ($\lambda = 2$, $\phi = 0.5$).
 (40) For solvents (segments) with less than C_3 symmetry, specification of the average orientation of the molecule relative to the constraint requires more than one element of the order matrix \mathbf{S} . In principle, only two parameters are necessary (if \mathbf{S} is diagonalized) but, in practice, the property considered is usually a tensor (α) and is not always diagonal in the frame that diagonalizes \mathbf{S} . In general, the polarizability along the constraint direction α_{zz} is given by $\alpha_{zz} = \frac{1}{3} \text{Tr } \alpha + \frac{2}{3} \sum_{\alpha\beta} \alpha_{\alpha\beta} S_{\alpha\beta}$.
 (41) Jarry, J. P.; Monnerie, L. *J. Polym. Sci.* **1980**, *18*, 1879.
 (42) Bullough, R. K. *J. Polym. Sci.* **1960**, *46*, 517.
 (43) Samulski, E. T. Proceedings of the International Symposium on Phase Transitions in Polymers, Case Western Reserve University, Jun 11-13, 1980. *Ferroelectrics* **1980**, *30*, 83.
 (44) Picot, C., et al. *Macromolecules* **1977**, *10*, 436 and references cited therein.

Carbon-13 Nuclear Magnetic Resonance Studies of Solid Segmented Copolymers. 1. Mobile Domains of a Polyester Thermoplastic Elastomer

Lynn W. Jelinski,* F. C. Schilling, and F. A. Bovey

Bell Laboratories, Murray Hill, New Jersey 07974. Received December 4, 1980

ABSTRACT: ^{13}C NMR was used to characterize the molecular motions which occur in the mobile regions of solid Hytel thermoplastic elastomer, a segmented copolymer composed of tetramethylene terephthalate "hard" segments and poly(tetramethyleneoxy) terephthalate "soft" segments. The samples studied range from 0.96 to 0.80 mole fraction hard segments. Proton scalar decoupled ($\gamma H_2/2\pi = 4$ kHz or 1 G) ^{13}C NMR spectra were observed in the solid state for all Hytel samples but not for the poly(butylene terephthalate) homopolymer. The fraction of each sample which contributes to the scalar-decoupled spectrum was found to consist of all of the aliphatic carbons of the soft segments and $\sim 10\%$ of the terephthalate and hard-segment carbons. The soft-segment aliphatic carbon line widths are a linear function of the average hard block length of the polymer but are essentially independent of temperature over the range 30–110 $^\circ\text{C}$. The T_1 values are identical for both soft-segment aliphatic carbons and are independent of the mole fraction of hard segment in the polymer. The T_1 values increase with increasing field strength and with increasing temperature. The NOE values at 47 kG for the soft-segment OCH_2 and $\text{CH}_2\text{CH}_2\text{CH}_2\text{CH}_2$ carbons are also independent of the hard-segment content of the polymer. Taken together, these data indicate that the part of the dipolar Hamiltonian made time dependent by anisotropic thermal motion is independent of the hard-segment content of the polymer. However, the angular range over which reorientation occurs is directly related to the average hard block length. These results support a model for Hytel structure in which there is phase separation and in which there is negligible mixing of the two phases at the domain boundaries.

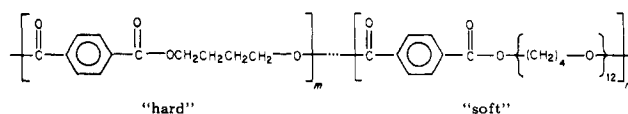
Introduction

Block copolymer thermoplastic elastomers generally contain amorphous "soft" segments and structured "hard" segments which are not miscible. The chemical incompatibility of the two segments results in phase separation, from which the unique mechanical and thermal properties of these polymers derive. The soft segments impart elastomeric character to the polymers, whereas the hard segments form thermally reversible noncovalent networks analogous to the covalent cross-links in elastomers. The hard-segment networks rely on various intramolecular interactions for their stability: the hard segments of the polyurethanes are stabilized by hydrogen bonding,¹ the styrene-butadiene or -isoprene block copolymer hard segments contain polystyrene in the glassy phase,² the ionomer resins rely upon ion clusters in the hard phase for their structural stability,^{3,4} and the polyester hard segments form a network of crystalline lamellar regions.⁵

Although the nature of the microphase separation,⁶ the dynamic interactions between the chains in the hard and soft phases,^{2,7,8} and the composition of the domain boundaries⁹ in the polyurethanes, the polystyrene-butadiene, and the polystyrene-isoprene systems have been the

subjects of recent active study, the polyester class of block copolymers seems to have escaped a similar systematic examination.⁵

Hytel is a thermoplastic polyester elastomer produced by E. I. du Pont de Nemours and Co. and is available in a range of compositions of m tetramethylene terephthalate hard segments and n poly(tetramethyleneoxy) terephthalate soft segments.



Hytel is formed by the melt transesterification of dimethyl terephthalate, 1,4-butanediol, and poly(tetramethylene ether) glycol, the latter having a number-average molecular weight of about 1000.¹⁰ The distribution of the copolymer blocks is assumed to be random.^{5,11}

Electron microscopy has shown that these copolymers exhibit a two-phase morphology.^{5,12,13} However, the structure consists of continuous and interpenetrating crystalline and amorphous phases,⁵ rather than the discrete domain structure which is seen for styrene-butadiene or

-isoprene copolymers.²⁶ The results from wide-angle X-ray diffraction indicate that the hard segments of drawn Hytrel have the same structure as the drawn tetramethylene terephthalate homopolymer.⁵ However, the degree of crystallinity determined by wide-angle X-ray diffraction has been shown to be a function of the thermal history of the sample.¹¹

Thermal analysis also supports the existence of a two-phase structure.^{5,11,14-16} However, both the glass transition temperature of the amorphous phase and the melting temperature of the crystalline phase increase with increasing hard-segment content of the polymer.⁵ These results have been interpreted to indicate that some of the hard-segment units reside in the elastomeric phase.⁵ Although the thermograms are a function of the thermal history of the sample, they indicate that the crystalline domains of Hytrel polymers with large amounts (~50 wt %) of soft segments contain a variety of crystal imperfections.¹¹

We report here the results of ¹³C NMR investigations of Hytrel in solution and of solid Hytrel, using scalar decoupling. These experiments, in conjunction with a solid-state ¹³C NMR study,¹⁷ are directed at obtaining a better understanding of the molecular motions which occur in both the amorphous and crystalline domains in the bulk copolymer, and thereby a clearer picture of the nature of the phase separation and the character of the domain boundaries.

¹³C NMR spectroscopy is a technique particularly well suited to the study of molecular motions in polymers.¹⁸ Because the naturally abundant ¹³C nuclei are relatively well isolated in the lattice, the relaxation rates of individual carbons are determined primarily by the local environment and are not, in general, equalized by spin diffusion. The ¹³C resonances of interest must, of course, be separately observable. This can be achieved by ordinary high-resolution NMR techniques for most polymers in solution because the dipolar interactions and the chemical shift anisotropy are generally averaged by rapid motion of the polymer.^{19,20} Individual ¹³C NMR resonances may be resolved in the solid state by combinations of magic-angle spinning, dipolar decoupling, and cross polarization.^{17,21} Alternatively, these resonances may be detected by ordinary high-resolution ¹³C NMR techniques (i.e., scalar decoupling) if some of the carbons in the polymer undergo motions which are fast compared to the static dipolar interaction (~10⁴–10⁵ Hz) and if these motions cause reorientation over a large enough range of solid angle.²⁰ (Throughout this paper we will use the term "scalar decoupling" to designate the ca. 4-kHz proton noise modulated radio-frequency field normally used to remove the ¹H–¹³C *J* coupling in ¹³C NMR spectra of molecules in solution. The term "dipolar decoupling" refers to the ca. 45-kHz proton field used to remove static ¹H–¹³C dipolar interactions in solids.)

The ¹³C NMR results reported here provide direct evidence that all of the soft segments and a portion of the hard segments in Hytrel are mobile on the time scale of the static dipolar interaction, independent of the hard-segment content of the polymer. Line width measurements, scalar-decoupled magic-angle spinning experiments, variable-temperature studies, *T*₁ measurements, and nuclear Overhauser enhancements (NOE) are reported for the mobile carbons of Hytrel samples of known hard-segment content.

Experimental Section

Samples. Hytrel types 7246, 6346, 5526, and 4056 were obtained in both powder and pellet forms from du Pont. Polyether

glycol (Teracol 1000) was also obtained from du Pont. Eastman Chemicals provided the poly(butylene terephthalate) samples. All samples were employed as received.

NMR Spectra. ¹³C NMR spectra were recorded either at 21 kG on a Bruker WH-90 spectrometer (22.62 MHz for ¹³C) or at 47 kG on a Varian XL-200 spectrometer (50.3 MHz for ¹³C). The 90° pulse width for both probes was ca. 12 μs.

Polymer samples in the form of powder or chopped pellets were packed in 10-mm NMR tubes into which a capillary containing benzene-*d*₆, ethylene-*d*₄ glycol, or acetone-*d*₆ (for reference and field frequency lock) was inserted. Some spectra were run in the unlocked mode on the XL-200 (estimated drift <0.01 ppm/h). Scalar-decoupled spectra of the solid samples were recorded in a 12-kHz spectral window with 4K or 8K time domain data points. The number of accumulations and the pulse repetition rates are listed in the figure legends. The strength of the proton decoupling field ($\gamma H_2/2\pi$) was determined by using either ethylene glycol or dioxane and was adjusted to 4 kHz (1 G).

Solution-state spectra were obtained on 15–20 wt % solutions of the polymers in hexafluoroisopropyl alcohol at 34 °C or in *m*-cresol at 100 °C, using a 10-kHz spectral window and 16K time domain data points. An internal capillary of benzene-*d*₆ or ethylene-*d*₄ glycol was used for field frequency lock and reference purposes.

Variable temperature was achieved by using the standard spectrometer accessories. The temperature controller was calibrated by using the proton shifts of ethylene glycol. The temperatures are considered accurate to ±2 °C. The samples were generally equilibrated in the probe at the desired temperature for 30–60 min prior to data accumulation.

***T*₁ Measurements.** *T*₁ values were measured by using a 180°–*t*–90°–*T* inversion–recovery pulse sequence²⁷ with continuous proton saturation. The optimum 180° pulse width was determined prior to each measurement. The time between pulse sequences was 2 s at 21 kG and 3 s at 47 kG. Measurements were generally made for 10–12 values of *t* which ranged from 0.005 s to *T*. Both integrated peak intensities and peak heights were used for the analysis of each *T*₁ data set; equivalent results were obtained in both cases. Plots of the data showed deviation from single-exponential behavior at long values of *t*. Consequently the *T*₁ values were taken from a least-squares analysis of the points out to (2–3)*T*₁ in order to avoid cross-correlation contributions to the relaxation times.²⁸

Nuclear Overhauser Enhancements. Nuclear Overhauser enhancements (1 + η) were measured by the gated decoupling technique.²⁹ The pulse repetition rate for both the Overhauser-suppressed and Overhauser-enhanced spectra was 8 s. Peak integrations were used to determine the NOE.

Quantification by NMR. The values of *m* and *n* for each of the Hytrel polymer samples were measured by solution-state ¹³C NMR (see above NMR Spectra section). Spectra were accumulated with a 30-s recycle delay time, using gated decoupling to suppress the NOE. The free induction decays were zero-filled prior to transformation. The peaks were cut out and weighed. The results for the pellet and powder samples were identical.

The fraction of each solid sample which contributes to the scalar-decoupled signal intensity was determined by comparison of the Overhauser-suppressed signal intensity obtained from a known weight of the polymer with the signal intensity from a known weight of ethylene glycol.³⁰ The samples were of the same volume and occupied the same position in the receiver coil. Probe tuning was optimized for each sample. The intensities were measured both by digital integration and by cutting and weighing the peaks. Identical results were obtained in both cases.

Results and Discussion

Determination of the Mole Fraction of Hard and Soft Segments in Hytrel Samples. The aliphatic region of the ¹³C NMR spectrum of Hytrel in solution (Figure 1) consists of resonances at 26.8 and 71.3 ppm (B and D), which are unique to the soft segments, and at 25.9 and 66.1 ppm (A and C), which arise primarily from the hard segments but contain small contributions from the carbons of the soft segments which flank the terephthalate groups. The assignments were made on the basis of the ¹³C NMR

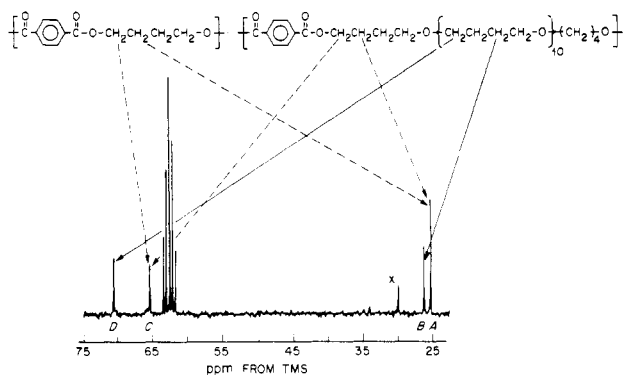


Figure 1. Methylene region of 50.3-MHz ^{13}C NMR spectrum of Hytrel 6346 (15 wt % in *m*-cresol, 100 °C, 30-s recycle delay, 256 accumulations, gated decoupling) illustrating the assignment of aliphatic resonances for the purpose of measuring the mole fraction of hard and soft segments. The peak marked with \times is due to an impurity in the solvent; the quintet arises from ethylene- d_4 glycol.

Table I
Mole Fraction and Weight Percent Hard Segments in Hytrel Samples Determined by ^{13}C NMR

Hytrel sample	mole fraction hard ^a	wt % hard ^b	average hard block length, ^c units
4056	0.80	44	6
5526	0.87	57	8
6346	0.94	75	17
7246	0.96	81	22

^a Each entry represents the average for at least two samples from different lots; estimated error $\leq \pm 0.01$.

^b The calculations are based on a number-average molecular weight of 1000 for the poly(tetramethylene ether) glycol. ^c Reference 5.

work of Komoroski³¹ on poly(butylene terephthalate) and by analogy to model compounds. The mole fraction of hard and soft segments can be calculated from such spectra, provided that spectral accumulation conditions are such that the A:C and B:D ratios are unity and that the average length of the poly(butylene ether) glycol is known. The average length of 12 was determined for poly(butylene ether) glycol by ^{13}C NMR. This value is in good agreement with the number-average molecular weight of 1000 reported by Wolfe.^{10,32} In view of the widely different NOE values and the factor-of-two difference in the methylene line widths reported by Komoroski for the poly(butylene terephthalate) homopolymer, the quantitative spectra reported here were obtained without an Overhauser enhancement. Under these conditions a 30-s recycle delay time was more than sufficient to obtain accurate intensities. We also observed a factor-of-two difference in the line widths of the methylene peaks A and C which was independent of the average hard block length of the sample.

Table I contains the results of ^{13}C NMR determination of the mole fraction of hard segments for a range of Hytrel samples. Those samples for which literature mole fractions have been reported (Hytrel 4056)¹¹ or can be inferred (Hytrel 5526)⁵ are in excellent agreement with the values reported here.

Scalar-Decoupled ^{13}C NMR Spectra of Solid Hytrel.

A. Determination of the Fraction of Each Sample Which Contributes Intensity to the Scalar-Decoupled Spectrum. All of the Hytrel samples examined by ^{13}C NMR have spectra which are observed by scalar decoupling ($\gamma H_2/2\pi = 4$ kHz) (Figure 2a-d) whereas poly(butylene terephthalate) does not (Figure 2e). These results

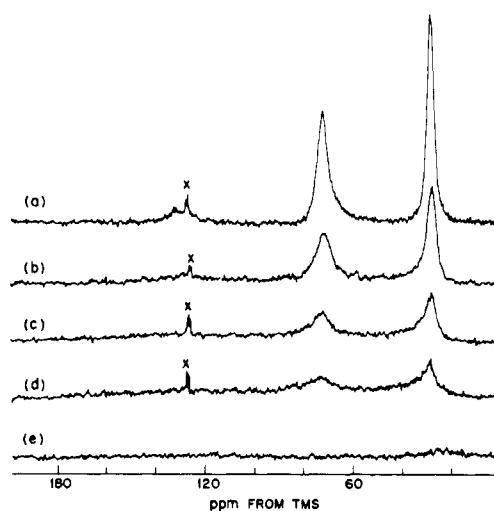


Figure 2. Scalar-decoupled ($\gamma H_2/2\pi = 4$ kHz) 50.3-MHz ^{13}C NMR spectra of solid Hytrel and poly(butylene terephthalate): (a) Hytrel 4056; (b) Hytrel 5526; (c) Hytrel 6346; (d) Hytrel 7246; (e) poly(butylene terephthalate). All spectra were obtained on the same amount of polymer and were recorded at 34 °C with 1024 accumulations and a 3-s pulse repetition rate. All spectra are plotted on the same vertical scale with 5 Hz of digital filtering. The peaks marked with \times arise from an internal capillary containing benzene- d_6 .

are not surprising in view of the molecular motion observed for some residues in other segmented copolymers (the styrene-isoprene diblock copolymers² and the polyurethanes^{8,6}) and the lack of motion implied by the crystal structure of poly(butylene terephthalate).^{33,34} However, through a combination of conventional and solid-state ^{13}C NMR techniques¹⁷ we are able to determine which, and how many, of the hard- and soft-segment carbons are mobile on the time scale of the ^{13}C - ^1H dipolar interaction ($\sim 10^4$ - 10^5 Hz).

The spectra of solid Hytrel (Figure 2) contain two well-resolved resonances at 29 and 73 ppm in addition to a broad aromatic and carbonyl region. It is well-known that chemical shifts in the solid and liquid states are not necessarily identical.^{21,35} Therefore, in order to prove that the scalar-decoupled 73-ppm peak arises primarily from the soft-segment carbons, it is necessary to obtain spectra of the solid samples under conditions where the hard-segment OCH_2 carbons could be observed. The residual line broadening for the carbons detected by scalar decoupling (residual dipole-dipole interactions and incompletely averaged chemical shift anisotropy) can be removed by magic-angle sample spinning²¹ while performing the standard scalar-decoupling Fourier transform NMR experiment. The results of such an experiment are shown in Figure 3a. The 29- and 73-ppm resonances peaks have been narrowed from 161 and 245 Hz, respectively, to 51 and 58 Hz, thereby eliminating overlap with the OCH_2 resonances of the hard segment, if present. Shown for comparison in Figure 3b is the corresponding spectrum from the dipolar-decoupled magic-angle spinning experiment in which all of the carbon resonances are observed. (The intensities of the peaks arising from the hard-segment carbons are not reliable due to T_1 differences among the carbons.¹⁷) These spectra illustrate that the methylene carbons of the hard segments contribute little signal intensity to the scalar-decoupled spectrum. The scalar-decoupled signal intensity therefore arises primarily from the aliphatic carbons of the poly(butylene ether) chains but contains contributions from the terephthalate residues.

The fraction of the samples which contributes to the scalar-decoupled signal intensity can be quantified by

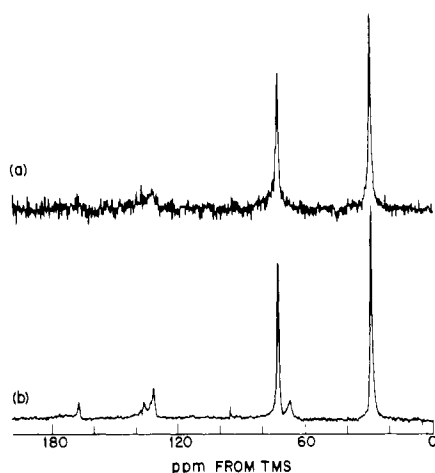


Figure 3. Scalar-decoupled (a) and dipolar-decoupled (b) 50.3-MHz Overhauser-suppressed ^{13}C NMR spectra of solid Hytrel 4056 spinning at 1.9 kHz at the magic angle. Both spectra were obtained with a 1-s recycle delay and have been scaled to compensate for differences in the number of accumulations.

comparing the signal intensity from a known weight of polymer to the signal intensity from a known weight of ethylene glycol³⁰ (see Experimental Section). The data indicate that the number of mobile carbons exceeds the number of soft carbons by $\sim 10\%$ for all samples. On the basis of the magic-angle spinning experiments (see above), we must conclude that the additional mobile carbons come largely from the terephthalate groups.

Integration of a scalar-decoupled spectrum of solid Hytrel 4056 of high signal-to-noise ratio gives relative intensity ratios for the (aromatic plus carbonyl): OCH_2 : $\text{CH}_2\text{CH}_2\text{CH}_2\text{CH}_2$ regions of 1:2:2. Calculations involving this ratio, the number of carbons observed by scalar doubling, and the solution data in Table I fit very well with a model in which all of the poly(butylene ether) carbons and the carbons of the terephthalate groups on both sides of the polyether segment contribute to the scalar-decoupled ^{13}C NMR signal intensity. Another model which fits the data equally well is one in which the scalar-decoupled signal intensity comes from all of the soft-segment carbons (terephthalate groups included) plus $\sim 10\%$ of the hard segments which are not fully incorporated in the crystalline lamellar domains. Given the nature of the experiments, a more quantitative interpretation is not warranted. However, it is clear from these data that the scalar-decoupled spectra contain more intensity in the carbonyl/aromatic region than predicted by the chemical composition (Table I) of the soft segments alone. These results suggest that the terephthalate groups which form the covalent portion of the domain boundaries are involved in rapid anisotropic molecular motions ($\tau_c \lesssim 10^{-5}$ s). Additional data (see below) suggest that the local motions of soft residues near (but not covalently bonded to) the domain boundaries are not influenced by the crystalline domains. In this respect, these results support phase separation and imply that the boundaries between the domains are sharp.

B. ^{13}C NMR Line Widths for the Mobile Aliphatic Carbons of Hytrel. The line widths measured for Hytrel samples at two magnetic field strengths are listed in Table II. The line widths exhibit a complex field strength dependence. On the basis of these data it is certain that the motions of these carbons are not in the extreme narrowing regime. The line widths observed here are of intermediate value. They can be compared to the ~ 25 -Hz scalar-decoupled line widths observed for the mobile methylene

Table II
 ^{13}C NMR Line Widths^a for the
Mobile Aliphatic Carbons of Solid Hytrel (Hz)

sample	29-ppm resonance		73-ppm resonance	
	21 kG	47 kG	21 kG	47 kG
4056	75	161	117	245
5526	112	211	176	276
6346		~ 360		~ 470
7246	~ 340	~ 500	~ 500	~ 1000

^a The line width was taken as the full width at half-maximum height. These values include 5 Hz of line broadening. All spectra were recorded at 34 $^\circ\text{C}$; estimated uncertainty $\pm 5\%$.

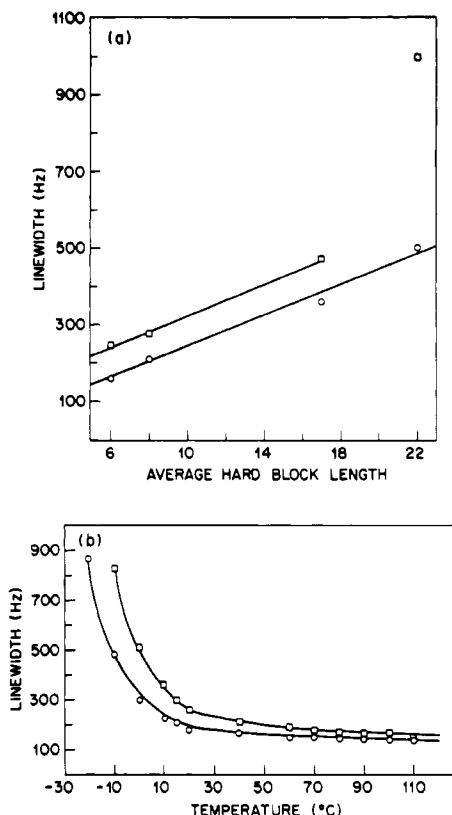


Figure 4. Line widths of the ^{13}C NMR (50.3 MHz) solid Hytrel scalar-decoupled 29-ppm resonance (O) and the 73-ppm resonance (\square) (a) as a function of average hard block length at 34 $^\circ\text{C}$ and (b) as a function of temperature for Hytrel 4056.

carbons in styrene-isoprene diblock copolymers at 22.6 MHz² and to the 500–900-Hz scalar-decoupled line widths observed for the amorphous carbons in linear polyethylene at 67.9 MHz.²²

The scalar-decoupled Hytrel $\text{CH}_2\text{CH}_2\text{CH}_2\text{CH}_2$ resonance at 29 ppm is narrower than the OCH_2 resonance at 73 ppm for all samples studied and at both field strengths. This difference in line width may be due to additional modes of low-frequency motion available to the central carbons of the butylene units which do not occur for the oxygen-linked carbons. Alternatively, the chemical shift anisotropies for these two types of carbons may be unequal. Both carbon line widths, however, exhibit a linear dependence on the average hard block length of the polymer (Figure 4a). One can interpret this correlation by determining the major sources which contribute to the scalar-decoupled line width.

Magic-angle sample spinning at 1.9 kHz (in conjunction with the conventional scalar-decoupling experiment) reduces the line width from 161 and 245 Hz (Figure 2a) to

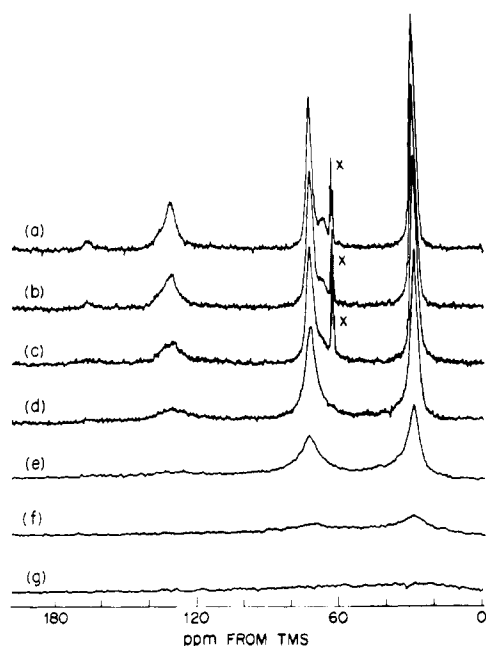


Figure 5. Scalar-decoupled 50.3-MHz ^{13}C NMR spectra of bulk Hytrel 4056 as a function of temperature: (a) 110; (b) 90; (c) 60; (d) 20; (e) 0; (f) -20; (g) -30 °C. Each spectrum represents 1024 Overhauser-enhanced transients acquired with a 3-s recycle delay. The peak marked with \times in the high-temperature spectra is from ethylene- d_4 glycol in a capillary.

51 and 58 Hz (Figure 3a) of the respective 29- and 73-ppm resonances of Hytrel 4056. Therefore, residual dipolar interactions and chemical shift anisotropy are the primary sources of line broadening, since both the dipolar interaction and the chemical shift anisotropy exhibit a $3 \cos^2 \theta - 1$ dependence under rigid-body rotation^{21,36} (where θ is the angle between the rotation axis and the external magnetic field). Static spectra of Hytrel obtained with double the decoupling power (i.e., $\gamma H_2/2\pi = 8$ kHz) show no further reduction in line width. (Static dipolar-decoupled ($\gamma H_2/2\pi \sim 50$ kHz) spectra are actually broader than the scalar-decoupled spectra because the rigid carbons which now contribute intensity to the spectra overlap the resonances of the mobile carbons.) In addition, fully coupled static spectra of Hytrel 4056 and Hytrel 7246 retain >95% and >80%, respectively, of the scalar-decoupled spectral intensity, although the spectra are broadened. Finally, a magic-angle spinning spectrum (1.9 kHz) of Hytrel 4056 with no decoupling contains lines which are as narrow as those of Figure 3a. (The bases of the peaks show broadening, presumably due to the part of the scalar coupling tensor which is not removed by magic-angle spinning³⁶ and due to residual dipolar interactions experienced by some of the mobile carbons.) These results suggest that the motions of the carbon in the amorphous regions of Hytrel are both rapid on the time scale of the dipolar interaction and anisotropic. The internuclear C-H vectors are unable to reorient completely over all range of solid angle and thus have nonvanishing dipolar and chemical shift interactions. Furthermore, the angular range over which reorientation occurs does not appear to be uniform for all carbons of the soft segments.

These results, in conjunction with the linear dependence of the line width on the average hard block length of the polymer (Figure 4a), suggest that the hard segments restrict the angular range over which both directly attached butylene units and internal butylene units in the domain boundaries can reorient. An alternate explanation, where the domain boundaries are assumed to consist of a mixed

Table III
 ^{13}C NMR T_1 (s) and Nuclear Overhauser Enhancements for the Mobile Aliphatic Carbons of Hytrel^a

Hytrel sample	NOE at 47 kG ^b		T_1 at 47 kG ^c		T_1 at 21 kG ^c	
	29 ppm	73 ppm	29 ppm	73 ppm	29 ppm	73 ppm
4056	2.3	2.1	0.21	0.22	0.12	0.12
5526	2.0	1.8	0.20 ^d	0.21 ^d	0.14	0.12
6346	2.3	1.9	0.20	0.24		
7246			0.21	0.21		

^a Recorded at 34 °C unless noted otherwise. ^b Values are reported as $1 + \eta$; estimated uncertainty ± 2 .

^c Determined by inversion-recovery; estimated uncertainty ± 0.02 s. ^d T_1 at 75 °C is 0.43 s.

phase of hard and soft segments, does not fit these data and is further argued against by the temperature independence of the line widths of the carbons of the mobile regions (see below).

Representative temperature-dependent scalar-decoupled ^{13}C NMR spectra of Hytrel 4056 ($T_m = 180$ °C;^{5,10} $T_g = -70$ °C⁵) are shown in Figure 5. As the temperature is raised, the OCH_2 resonance at ~ 70 ppm, due presumably to those hard-segment residues which are too short to crystallize, is narrowed. As the temperature is decreased below ~ 10 °C, the lines broaden rapidly. (These phenomena are reversible with temperature.) A plot of the line width as a function of temperature is shown in Figure 4b. The line width for the 73-ppm OCH_2 resonance shows a minimal variation over the temperature range ~ 40 – 110 °C. The line width of the 29-ppm $\text{CH}_2\text{CH}_2\text{CH}_2\text{CH}_2$ resonance exhibits similar behavior over the temperature range ~ 20 – 110 °C. The sharp increase of the line widths observed below ~ 10 °C (Figure 4b) is attributed to dipolar broadening which accompanies the onset of motions which have frequencies in the range of $\sim 10^5$ Hz. T_1 measurements (see below) indicate that the rate of motion of these carbons increases with increasing temperature. These line width measurements indicate, however, that the angular range of solid angle sampled by reorientation of the soft segments does not change appreciably over an ~ 80 °C change in temperature. These results support the view that the presence of rigid domains prohibits complete reorientation of the soft segments but that the rate of motion in the mobile domains (reflected by that part of the dipolar Hamiltonian rendered time dependent by these motions) is independent of the amount of hard segment in the polymer. Thus, the mobile and rigid domains appear to have sharp, well-defined boundaries, rather than the continuum expected if large amounts of mixed phases exist.

C. Relaxation Measurements for the Mobile Aliphatic Carbons of Hytrel. The T_1 and NOE values for Hytrel samples are listed in Table III. The predominant relaxation is assumed to be dipolar due to the presence of two directly bonded protons on each carbon and by analogy to polymer models.³⁷ The increase in the T_1 values both with increasing field strength and with increasing temperature indicates that the motions which determine the T_1 are on the fast correlation time side of the T_1 curve, but not fast enough to be in the motional narrowing regime. As expected, the data do not fit a single correlation time model.³⁸ In view of the anisotropy of the motions demonstrated by the line widths, a distribution of isotropic correlation times³⁹ is also an inadequate description of the motional dynamics of the system. A comprehensive analysis of the rate and angular range of these anisotropic carbon motions can probably best be performed by a

solid-state ^2H NMR line shape study. In the absence of such data, a quantitative analysis of these ^{13}C relaxation data would be premature. However, several conclusions may be drawn from a qualitative inspection of these data.

The T_1 values at both field strengths and for both carbons are independent of the hard-segment content of the polymer (Table III). The T_1 is determined primarily by local chain motions, and the rate of these motions does not appear to be influenced by the presence of large amounts of hard segments in the polymers. A similar invariance in T_1 values has been observed by Schaefer for carbon-black filled *cis*-polyisoprene²³ and also by Mandelkern and co-workers for the amorphous carbons of polyethylene in the presence of various amounts of crystalline polymer.²² However, unlike Hytrel, the polyethylene line width is a strong function of temperature.²²

In contrast to the T_1 , the NOE values for the two carbon resonances in Hytrel are not identical (Table III), although they both appear to be largely independent of the hard-segment content of the sample. Intermediate NOE values such as these are rapidly changing functions of the effective correlation time and therefore tend to be a more sensitive monitor of molecular motion than the T_1 . The NOE values suggest that the molecular motions of the OCH_2 carbons may be slightly slower than those of the $\text{CH}_2\text{CH}_2\text{CH}_2\text{CH}_2$ carbons. This interpretation is supported by the different low-temperature dependence of the line widths observed for these two carbons (Figure 4b).

Taken together, the relaxation data indicate that the rate of motions which occur in the amorphous domains is independent of the fraction of hard segment present in the polymer and, in this sense, suggest that phase separation is fairly complete. It should be noted, however, that the T_1 and NOE values of a system such as Hytrel are weighted by those motions which occur at or near the Larmor frequency and may not accurately reflect the motions of the polymer as a whole.

Summary

Solution-state NMR can be used to quantify the mole fraction of hard and soft segments in Hytrel samples. Once these mole fractions are known, the results of the scalar-decoupled ^{13}C NMR experiments on solid Hytrel samples can be interpreted in terms of phase separation, the composition of the domain boundaries, and the dynamical interactions within the amorphous region.

The ^{13}C NMR line widths for the mobile carbons in Hytrel are a linear function of the hard-segment content of the polymer but are essentially temperature independent over a $\sim 100^\circ\text{C}$ range in temperature. Scalar-decoupled magic-angle spinning experiments indicate that the major sources of line broadening are residual dipolar interactions and chemical shift anisotropy. The presence of hard segments in the polymer samples prevents the mobile carbon C-H internuclear vectors from sampling all values of solid angle. Relaxation parameters (T_1 and NOE) indicate that the rate of motion of the mobile carbons of the soft segments is independent of the hard segments present in the polymer.

The ^{13}C NMR line widths and relaxation parameters, together with quantification experiments, support a model for Hytrel domain structure in which the rigid and

amorphous domains are phase separated and in which there is negligible mixing of the two phases at the domain boundaries.

Acknowledgment. We are grateful to Mr. J. G. Hedberg of du Pont, who kindly provided us with the powdered Hytrel samples, and to colleagues T. K. Kwei, D. C. Douglass, and T. M. Duncan for helpful discussions.

References and Notes

- (1) Senich, G. A.; MacKnight, W. J. *Macromolecules* **1980**, *13*, 106.
- (2) Mor  se-S  g  la, B.; St-Jacques, M.; Renaud, J. M.; Prud'homme, J. *Macromolecules* **1980**, *13*, 100.
- (3) Marx, C. L.; Koutsky, J. A.; Cooper, S. L. *J. Polym. Sci., Part B* **1971**, *9*, 167.
- (4) Tobolsky, A. V.; Lyons, P. F.; Hato, N. *Macromolecules* **1968**, *1*, 515.
- (5) Cella, R. J. *Encycl. Polym. Sci. Technol., Suppl.* **1977**, *2*, 485.
- (6) Assink, R. A. *J. Polym. Sci., Polym. Phys. Ed.* **1977**, *15*, 59.
- (7) Wardell, G. E.; McBrierty, V. J.; Douglass, D. C. *J. Appl. Phys.* **1974**, *45*, 3341.
- (8) Assink, R. A. *Macromolecules* **1978**, *11*, 1233.
- (9) Kraus, G.; Rollmann, K. W. *J. Polym. Sci., Polym. Phys. Ed.* **1976**, *14*, 1133.
- (10) Wolfe, J. R., Jr. *Polym. Prepr., Am. Chem. Soc., Div. Polym. Chem.* **1978**, *19* (1), 5.
- (11) Hourston, D. J.; Hughes, I. D. *J. Appl. Polym. Sci.* **1977**, *21*, 3093.
- (12) Cella, R. J. *J. Polym. Sci., Polym. Symp.* **1973**, *C42*, 727.
- (13) Cella, R. J.; Buck, W. H. *Polym. Prepr., Am. Chem. Soc., Div. Polym. Chem.* **1974**, *15* (1), 159.
- (14) Shen, M.; Mehra, V.; Niinomi, N.; Koberstein, J. T.; Cooper, S. L. *J. Appl. Phys.* **1974**, *45*, 4182.
- (15) Nishi, T.; Kwei, T. K.; Wang, T. T. *J. Appl. Phys.* **1975**, *46*, 4157.
- (16) Nishi, T.; Kwei, T. K. *J. Appl. Polym. Sci.* **1976**, *20*, 1331.
- (17) Jelinski, L. W. *Macromolecules*, submitted.
- (18) Schaefer, J. In "Structural Studies of Macromolecules by Spectroscopic Methods"; Ivin, K. J., Ed.; Wiley: New York, 1976; pp 201-26.
- (19) Bovey, F. A.; Kwei, T. K. In "Macromolecules: An Introduction to Polymer Science"; Bovey, F. A., Winslow, F. H., Eds.; Academic Press: New York, 1979; pp 207-71.
- (20) Mehring, M. *NMR* **1976**, *11*.
- (21) Schaefer, J.; Stejskal, E. O. *Top. Carbon-13 NMR Spectrosc.* **1979**, *3*, 283-324.
- (22) Komoroski, R. A.; Maxfield, J.; Sakaguchi, F.; Mandelkern, L. *Macromolecules* **1977**, *10*, 550.
- (23) Schaefer, J. *Macromolecules* **1972**, *5*, 427.
- (24) Duch, M. W.; Grant, D. M. *Macromolecules* **1970**, *3*, 165.
- (25) Komoroski, R. A.; Mandelkern, L. *J. Polym. Sci., Polym. Symp.* **1976**, *54*, 201.
- (26) Fleming, W. W.; Sullivan, C. E.; Torchia, D. A. *Biopolymers* **1980**, *19*, 597.
- (27) Becker, E. D. "High Resolution NMR", 2nd ed.; Academic Press: New York, 1980; pp 232-7.
- (28) Werbelow, L. G.; Grant, D. M. *J. Chem. Phys.* **1975**, *63*, 4742.
- (29) Opella, S. J.; Nelson, D. J.; Jardetzky, O. *J. Chem. Phys.* **1976**, *64*, 2533.
- (30) Jelinski, L. W.; Torchia, D. A. *J. Mol. Biol.* **1980**, *138*, 255.
- (31) Komoroski, R. A. *J. Polym. Sci., Polym. Phys. Ed.* **1979**, *17*, 45.
- (32) Wolfe, J. R., Jr. *Adv. Chem. Ser.* **1979**, No. 179, 129.
- (33) Mencik, Z. *J. Polym. Sci., Polym. Phys. Ed.* **1975**, *13*, 2173.
- (34) Alter, U.; Bonart, R. *Colloid Polym. Sci.* **1976**, *254*, 348.
- (35) Lyster, J. R., Jr. In "Contemporary Topics in Polymer Science"; Shen, M., Ed.; Plenum: New York, 1979; Vol. 3, pp 143-213.
- (36) Andrew, E. R. *Prog. NMR Spectrosc.* **1972**, *8*, 1.
- (37) Lyster, J. R., Jr.; Horikawa, T. T. *J. Phys. Chem.* **1976**, *80*, 1106.
- (38) Allerhand, A.; Doddrell, D.; Komoroski, R. *J. Chem. Phys.* **1971**, *55*, 189.
- (39) Schaefer, J. *Macromolecules* **1973**, *6*, 882.